JOURNAL OF MATERIALS SCIENCE 28 (1993) 5814–5818

Thermal expansion and relaxation–crystallization kinetics of metallic glass $Co_{63}Ni_6Fe_4V_2Si_{10}B_{15}$

G. M. LIN
Department of Physics, Zhongshan University, Guangzhou 510275, People's Republic of China

J. K. L. LAI, G. G. SIU
Department of Applied Science, City Polytechnic of Hong Kong, Hong Kong

The conventional dilatometric technique is applied to study the thermal expansion of the metallic glass $Co_{63}(FeNi)_{10}V_2Si_{10}B_{15}$ with cylindrical samples rolled from ribbon. The heating-rate effect on expansion and differential thermal analysis (DTA) is investigated. The non-linear region of the temperature variation curves of relative elongation all show a broad peak and a distinct peak which correspond to those in DTA. The broad peak in DTA resolves into two peaks: the first one is associated with the glass transition which is interpreted as a quasi-first-order transformation. On comparing with X-ray diffraction analysis, the crystallization is determined to be a two-stage process in which Co(4F) precipitation is a controlling factor.

1. Introduction

Metallic glasses undergo devitrification when heated, resulting in marked variations in macroscopic properties. Structural relaxation and phase transitions of metallic glasses are usually studied using measurements of mechanical, electrical and magnetic quantities. For example, simultaneous measurements of internal friction, relative shear modulus and electric resistance of the metallic glasses a-$Pd_{77.5}Ni_6Si_{16.5}$, a-$Pd_{85.5}Si_{14.5}$, a-$Pd_{77.5}Cu_6Si_{16.5}$, a-$Fe_{40}Ni_{40}P_{12}B_8$ and a-$Pd_{80}Si_{20}$ resolve the glass transition and crystallization at very low heating rate and the nature of the glass transition in a heating process is studied [1].

The volume (thermal expansion coefficient) change in a heating process, usually a contraction (reduction) owing to densification, attracts a lot of attention since it provides clues to the microscopic mechanisms of structural relaxation and crystallization. However, except for the Pd–Ni–P and Pt–Ni–P series which are easily quenched to the glassy state and from which a cylindrical sample is readily made [2], special apparatus design is necessary for applying dilatometric techniques to the typical ribbon-shaped metal glasses, e.g. Fe–Ni base metal glass [3]. Correlations between physical quantities are made to clarify the micro-scale processes, using measurements of densities and Young's moduli [4], thermal expansion coefficients before and after crystallization [5, 6], length contraction during crystallization and in low-temperature relaxation [7], relative elongation and modulus change [8], and determination of kinetic parameters through dilatometric measurements [9].

Extensive studies of the thermal expansion of amorphous metal alloys show that dilatation measurement, when related to other characterization measurements, is essential for understanding the structural relaxation and crystallization of metal glasses. In this work, we study the process of relaxation and crystallization of the metallic glass $Co_{63}(FeNi)_{10}V_2Si_{10}B_{15}$, a Co-base amorphous alloy which possesses outstanding magnetic properties [10], by applying the conventional dilatometric technique. Thermal expansion is measured with a ribbon sample rolled into a cylinder. The heating-rate effect on thermal expansion is investigated and activation energies are determined. The thermal expansion coefficients before and after relaxation and the contraction rates are determined by thermal cycling. The dilatation measurements are related to differential thermal analysis (DTA) and X-ray diffraction (XRD) studies. On this basis, the structural relaxation is discussed with the model of degeneration of short-range order (SRO) [1] and crystallization is determined to be a two-stage process in which the precipitation of Co(4F) crystals is a controlling factor.

2. Experimental procedure

Metallic glass ribbon, 15 mm wide and 60 μm thick, was fabricated by melt-spinning. The nominal composition was $Co_{63}Fe_4Ni_6V_2Si_{10}B_{15}$ and XRD confirmed that the initial state of ribbon was amorphous. To overcome buckling instabilities of ribbon samples when loaded in compression, a new sample preparation was adopted: the 15 mm wide ribbon was rolled lengthwise for five turns into a cylinder, 15 mm high and 8 mm in diameter. The ribbon was fixed by point-welding and the top and bottom were trimmed by a electrical spark machine. The elongation of this cylinder was measured using a conventional compression dilatometer. A fused quartz bar exerted a compression

0022–2461

force of 8 N on the sample, whose creep could be negligible as shown from the results (next section). The quartz tube with the sample and quartz bar of the dilatometer were installed inside a tube furnace. The elongation of the sample was read by a micrometer. The sample temperature was monitored by a small thermocouple of 0.5 K accuracy, set within the sample cylinder. The resolution of the thermal expansion coefficient reached 0.5×10^{-6} K^{-1}. Experiments were carried out in the atmosphere. Calibration was performed using a pure iron sample.

This sample preparation makes conventional dilatometric techniques suitable for determining thermal expansivities of the common ribbon-shaped samples of metallic glass. It is simple and effective compared with special designs of apparatus proposed before [3, 7–9].

Dilatation measurements were made on the cylindrical sample of metal glass $Co_{63}(FeNi)_{10}V_2Si_{10}B_{15}$ with different heating rates within the range 2 to 30 K min^{-1}. Thermal expansion measurements were also made in thermal cycling to determine contraction rates and thermal expansion coefficients before and after relaxation and crystallization. A Perkin-Elmer 1700 was used for the DTA measurements and a diffractometer (Rigaku D/MAX 3A) with CuK_{α_1} radiation and scanning rate 2° min^{-1} was used for *in situ* high-temperature XRD studies.

3. Results

The temperature variation curves of the relative elongation $\Delta l/l_0$, where l_0 is the initial length of the cylindrical sample (15 mm) and $\Delta l = l - l_0$, is shown in Fig. 1a, b, c and d for four heating rates: 5.5, 9.0, 15 and 25 K min^{-1}, respectively. When the temperature is lower than 700 K, thermal expansion is linear with temperature. The normal thermal expansion results. When the temperature increases to above 700 K, the temperature dependence of thermal expansion turns non-linear and two thermal expansion peaks P_L and P_H are observed in each curve. The elongation slows down first so that the curves deviate from straight lines. It then decreases with temperature at the first peak temperature T_L and the contraction reaches a maximum (the minimum of elongation) at ~ 800 K. A broad peak P_L results between 700 and 800 K. The metal glass expands again when heating continues but elongation drops (the sample contracts) at the second peak temperature T_H. $\Delta l/l_0$ also reaches a minimum at an even higher temperature and resumes its increase later. A distinct peak P_H results. The curve of $\Delta l/l_0$ versus T shifts to a higher position when the heating rate increases, while both T_L and T_H shift to higher temperatures. Table I shows the effect of the temperature increase rate on the peak temperatures.

To understand physical processes occurring in thermal expansion, results of *in situ* XRD testing with a heating rate of 5 K min^{-1} are shown in Fig. 2: the XRD patterns were recorded at (a) 723, (b) 823 and (c) 923 K, each held for 1 min. State (a) is on the low-temperature side of the peak P_L and the sample is expanding non-linearly. The XRD pattern shows that

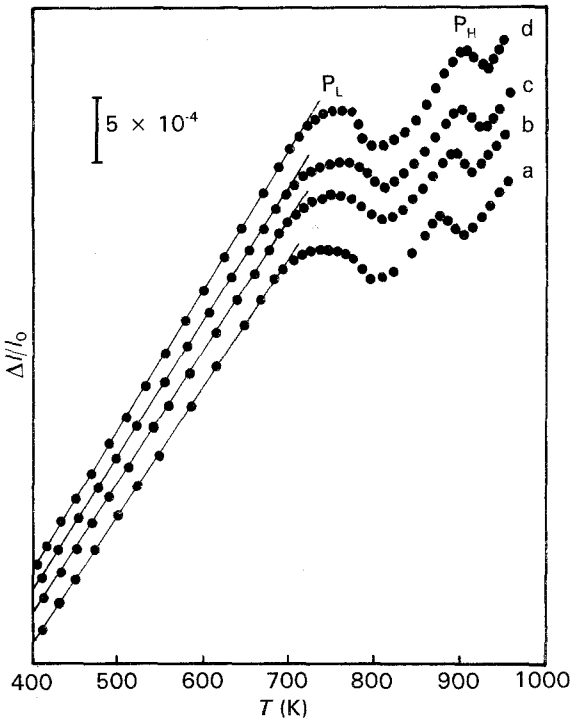

Figure 1 Heating-rate effect on thermal expansion of the metallic glass $Co_{63}Ni_6Fe_4V_2Si_{10}B_{15}$ at different heating rates: (a) 5.5, (b) 9.0, (c) 15, (d) 25 K min^{-1}.

a few small spikes begin to appear on the background-like halo pattern of the usual amorphous state. It can be concluded that the metal glass essentially maintains an amorphous state before any distinct pattern of crystal phase appears. However, tiny crystallites of less than 0.1 μm diameter may appear and also contribute to the background-like pattern. The non-linear expansion around P_L is hence related not only to structural relaxation but also to the beginning of crystallization. State (b) is in the valley between P_L and P_H. In the XRD pattern two crystalline phases, Co(4F) and Co_2Si, precipitate from the amorphous matrix but a partial amorphous phase still holds. This indicates that crystallization is in operation. The results of Fig. 2a and b show that the broad peak P_L involves both structure relaxation (glass transition) and crystallization (densification). On the low-temperature side, relaxation is the main process but on the high-temperature side, crystallization dominates over the former. State (c) is one of normal expansion, and crystallization completes. The XRD pattern shows a rapid increase of the content of the face-centred cubic phase Co(4F) and the precipitation of $Fe_{4.5}Ni_{18.5}B_6$, another crystalline phase. The distinct peak P_H results from the crystallization process only.

As a brief recapitulation of the above-mentioned results, the phase transition of the metal glass $Co_{63}Fe_6Ni_4V_2Si_{10}B_{15}$ in a heating process involves structural relaxation and crystallization. In the first stage, structural relaxation of amorphous metal alloy is the main process when the temperature is low but precipitation of Co(4F) and Co_2Si occurs in the high-temperature range. In the second stage, crystallization completes with further precipitation of Co(4F) and $Fe_{4.5}Ni_{18.5}B_6$. It is noticed that the lattice parameter of Co(4F) determined from the XRD is $a_0 = 0.345$ nm,

TABLE I Dependence on heating rate $\dot{T}$ of peak temperatures in thermal expansion and DTA curves

	Thermal expansion				DTA			
	5.5 K min^{-1}	9.0 K min^{-1}	15 K min^{-1}	25 K min^{-1}	5.0 K min^{-1}	10 K min^{-1}	15 K min^{-1}	25 K min^{-1}
T_G(K)					736.0	743.0	746.0	750.0
T_L(K)	754.0	763.5	773.0	778.5	762.0	774.0	778.5	788.5
T_H(K)	859.0	871.0	883.0	901.0	873.5	884.0	895.0	905.0

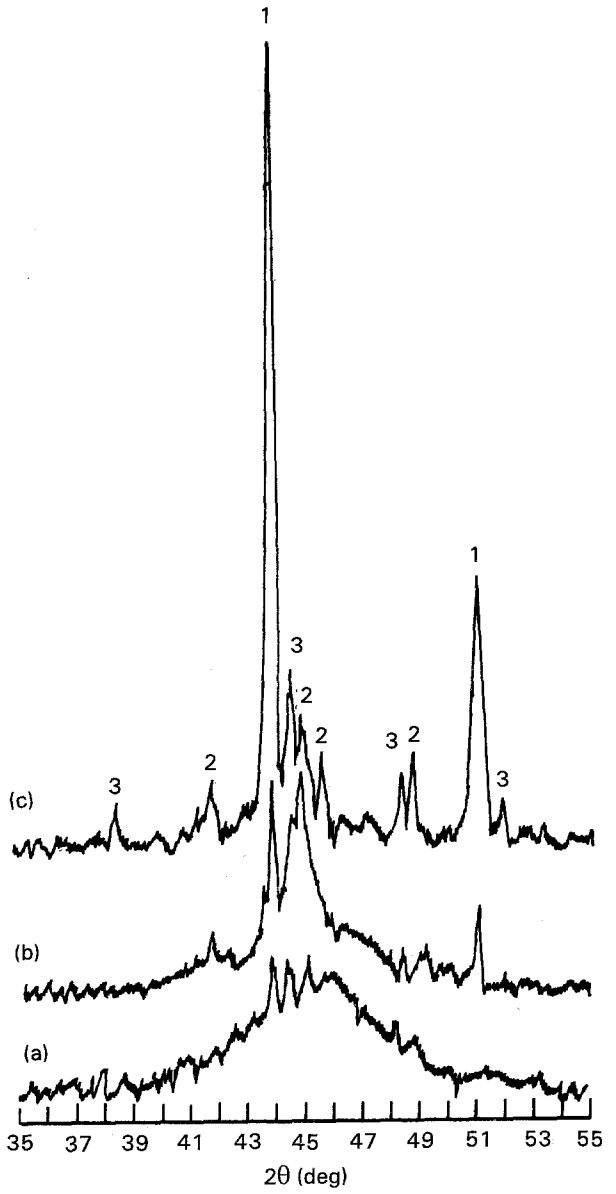

Figure 2 X-ray diffraction patterns at different relaxation and crystallization stages: (a) 723, (b) 823, (c) 923 K. (1) Co(4F), (2) Co_2Si, (3) $Fe_{4.5}Si_{18.5}B_6$.

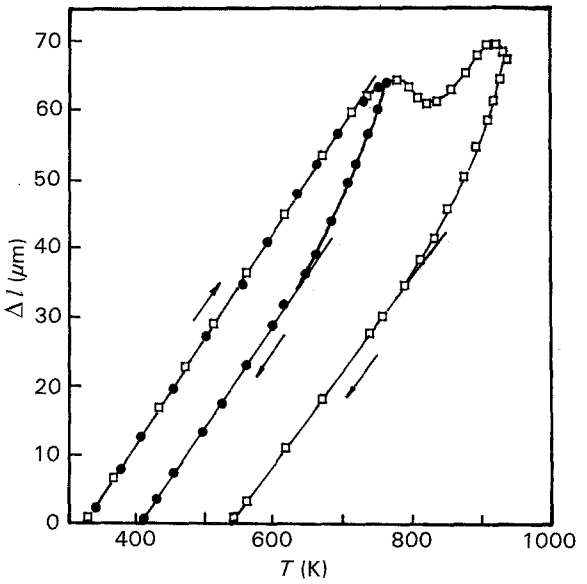

Figure 3 Thermal expansion curves of metallic glass sample under thermal cycling at a heating rate 25 K min^{-1} with maximum temperature (●) 723 and (□) 923 K.

3% larger than that of the ASTM standard card. It is likely that the dissolution of other atoms of the iron group of similar sizes and properties in the Co(4F) phase is the reason. To resolve glass transition and crystallization, further investigation is necessary.

Contraction occurs following structural relaxation or crystallization owing to densification. To determine the contraction rates and thermal expansion coefficients before and after phase transformation, thermal expansion measurements during thermal cycling were carried out and the results are shown in Fig. 3. Two thermal cycles at the same heating rate of 25 K min^{-1} reach maximum temperatures of 723 K (cycle I) and 923 K (cycle II), respectively, i.e. cycle I is performed at the end of relaxation and cycle II at the end of crystallization. Furnace cooling follows the heating. The metal glass shows irreversible changes in $\Delta l/l_0$ and the hysteresis of the cooling curve exhibits the length contraction of the sample. The length contraction rates are 0.066 and 0.154% for structural relaxation (cycle I) and crystallization (cycle II), respectively. The temperature rates of volumetric contraction [$\beta \approx 3\mathrm{d}\,(\ln l)/\mathrm{d}T$] are then 0.198 and 0.462% for relaxation and crystallization, respectively, so the total contraction rate is 0.66%. Our results are in agreement with published results, e.g. of the same order of magnitude as those of Pd–Cu–Si, Ni–P–B–Al and Fe–P–Si–Al (Table II of Chen [4]) and similar to what Kursumovic *et al.* [7] observed for the length contraction rates of $Fe_{20}Ni_{40}B_{20}$. The thermal expansion coefficient α is also obtained from Fig. 3. α for cycle I in heating is about the same as that in cooling, 10.5×10^{-6} K^{-1}, but α of cycle II decreases by 7.6% to 9.7×10^{-6} K^{-1} after crystallization.

DTA at different heating rates provides further information as shown in Fig. 4. The peaks P_L and P_H correspond to two endothermic peaks in heating. However, the DTA has a higher resolution than the expansion measurements: the peak P_L splits into peaks P_G and $P_{L'}$. The peak temperatures T_G, $T_{L'}$ and T_H all increase with heating rate $\dot{T}$ (Table I) as well as

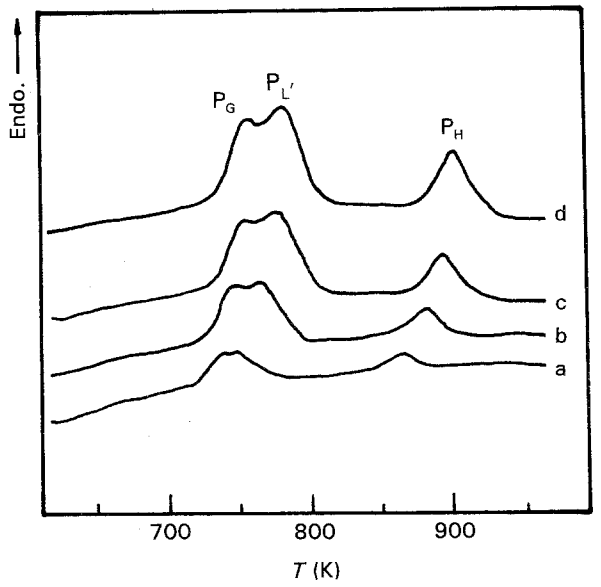

Figure 4 Heating-rate effect on DTA curves at different heating rates: (a) 5.0, (b) 10, (c) 15, (d) 25 K min^{-1}.

the splitting between P_G and $P_{L'}$. Fig. 5 shows the Kissinger graph of $\ln(\dot{T}/T_P^2 = -E_P/kR_P + \text{constant}$ [11] where the subscript p is for G, L and H, ΔE_p is the activation enthalpy of phase transition and k the Boltzmann constant. It is determined that $\Delta E_L = 3.27$ eV, close to $\Delta E_L = 3.19$ eV but more different from $\Delta E_G = 3.97$ eV; and ΔE_H(expan) = 3.32 eV, close to ΔE_H(DTA) = 3.18 eV. Besides, all values of T_H(DTA) are higher than T_H(expan), similar to $T_{L'} > T_L$. Hence we identify $P_{L'}$ with P_L.

It is noticed that the activation enthalpies ΔE_L and ΔE_H are essentially identical: $\Delta E_L = 3.19$ eV, $\Delta E_H = 3.18$ eV in DTA and $\Delta E_L = 3.27$ eV, $\Delta E_H = 3.32$ eV, in dilatation measurements. The average of ΔE_L and ΔE_H is 3.185 and 3.295 eV for DTA and dilatation measurements, respectively. The difference (0.11 eV) is caused by the experimental methods. Correlated with the XRD data, both P_L and P_H concern crystallization process and there should be only one identical activation enthalpy. Taking the average of the two methods, $\Delta E_X = 3.24$ eV $\pm$ 0.06 eV, where the subscript X is for crystallization.

The peak temperature T_G of the peak P_G (736 K at $\dot{T} = 5$ K min^{-1}) is comparable to 723 K in expansion experiments, which we take as the end of the structural relaxation in elongation and XRD measurements. The upward temperature shift in DTA ($\sim$10 K) compared with the elongation measurements (Table I) shows that this difference is not significant and is only caused by different experimental methods (sample size, detector etc.). Compared with the internal friction, relative shear modulus, resistivity and DSC investigations [1] in which the glass transition and crystallization are resolved, P_G is likely to be associated with the glass transition. The activation enthalpy $\Delta E_G = 3.97$ eV is considerably larger than ΔE_X, which shows that the physical mechanism is different.

From these experimental results, we conclude that non-linear thermal expansion of $Co_{63}Ni_6Fe_4V_2Si_{10}B_{15}$ starts with a glass transition and precipitation of Co(4F) and Co_2Si. These two processes

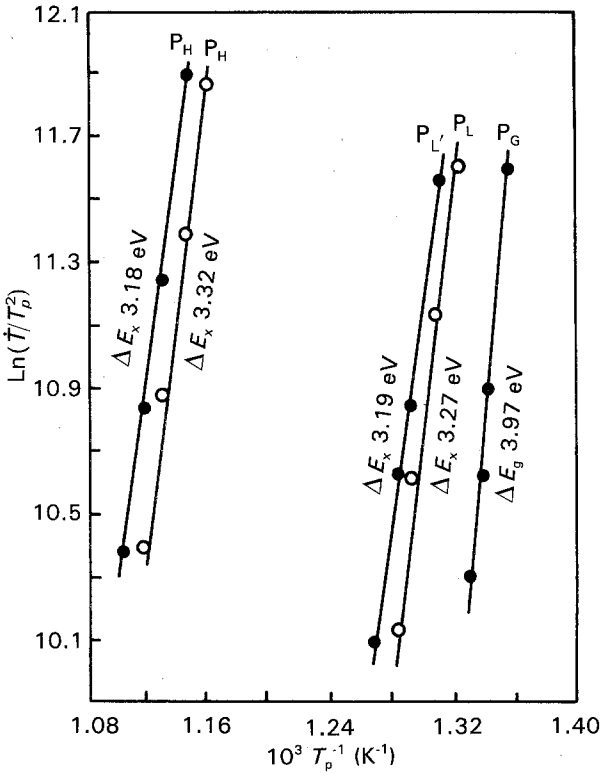

Figure 5 Kissinger graphs for (○) thermal expansion and (●) DTA data.

occur almost simultaneously at low heating rate but separate in the case of fast heating. Further crystallization occurs only after about 100 K with the precipitation of the crystalline phase $Fe_{4.5}Ni_{18.5}B_6$, which results in another peak of non-linear relative elongation. Endothermic peaks appear near the temperatures of the glass transition and two stages of crystallization. The height and the peak temperature of these peaks, in expansion or in DTA measurements, depend on the rate of temperature increase.

4. Discussion

The elongation measurements give similar results as previously reported. For example, the linearity of $\Delta l/l_0$ indicates that interatomic forces vary concurrently with the mean interatomic distances [8]. The contraction rates of relaxation and crystallization are of the same order of magnitude, which is likely to be related to a rather high degree of short-range order in metal glass compared with that in crystalline alloys [7].

Correlation between the elongation measurements, XRD and DTA provides further information on the relaxation–crystallization kinetics. The crystallization of $Co_{63}(FeNi)_{10}V_2Si_{10}B_{15}$ divides into two stages represented by P_L and P_H in which different crystalline phases precipitate but the precipitation of Co(4F) persists. The activation enthalpy of crystallization of this Co-based amorphous metal alloy is 3.24 eV, which is similar to but about 10% larger than the self-diffusion activation energy of cobalt. We conclude that the precipitation of Co(4F) is the controlling process in the crystallization of this metal glass.

The assignment of the peak P_G could be further verified by thermal cycling as carried out by Zhang

et al. [1]. The glass transition of a metal glass in heating is a glass→viscoelastomer transition and has been proposed as a quasi-first-order phase transformation [1]. The physical picture is the model of degeneration of SRO: a metal glass near the temperature T_G is an assembly of SRO clusters moving cooperatively, separated from each other by disordered films constructed from large atoms. On heating to a temperature lower than the crystallization one, the solid structure changes: the cluster size, degree of SRO and thus the solid-state viscosity reduce, and the cluster number increases. Partial chemical bond breaking follows and an endothermic peak appears. On the other hand, peaks P_L and P_H concern the nucleation of crystalline phases.

5. Conclusions

The dependence on the heating rate of the thermal expansion, DTA have been investigated for the metal glass $Co_{63}(FeNi)_{10}V_2Si_{10}B_{15}$. Resolution between the glass transition (structural relaxation) and crystallization is achieved. Compared with the results of XRD studies, crystallization of the metal glass is shown to be a two-stage process with different crystalline phases precipitated, in which the precipitation of Co(4F) is the controlling factor. The glass transition peak shown in DTA could be the same as the peak of quasi-first-order phase transformation investigated previously.

References

1. J. X. ZHANG, M. H. CHEN, D. M. LIN, G. G. SIU and M. J. STOKES, *J. Phys.: Condens. Mater.* **1** (1989) 9717.
2. H. S. CHEN, J. T. KRAUSE and E. A. SIGETY, *J. Non-Cryst. Solids* **13** (1973) 321.
3. H. A. BROOKS, *J. Appl. Phys.* **49** (1978) 213.
4. H. S. CHEN, *ibid.* **49** (1978) 3289.
5. J. E. SHELBY, *J. Non-Cryst. Solids* **34** (1979) 111.
6. J. STEINBERG, S. TYAGI and E. A. LORD Jr, *ibid.* **41** (1980) 279.
7. A. KURSUMOVIC, E. GIRT, B. L. BABIC, N. NJUHOVIC and B. LEONTIC, *ibid.* **44** (1981) 57.
8. K. BOTHE, M. HANSMAMN and H. NEUHAUSER, *Scripta Metall.* **19** (1985) 1513.
9. G. VLASÁK, P. DUHAJ, V. ŠVAJLENOVÁ and P. ŠVEC, *J. Non-Cryst. Solids* **99** (1988) 65.
10. X. L. WANG, G. Q. SUN, J. J. WANG, X. H. CHEN, Y. S. YANG and Y. G. LI, *IEEE Trans. Magn.* **18** (1982) 1188.
11. H. E. KISSINGER, *Anal. Chem.* **29** (1957) 1702.

Received 23 June 1992
and accepted 27 April 1993